



Aromatic Clusters as Potential Hydrogen Storage Materials

Ranita Pal¹ and Pratim Kumar Chattaraj^{2,3*}

¹Advanced Technology Development Centre, Indian Institute of Technology Kharagpur, Kharagpur, India, ²Department of Chemistry, Indian Institute of Technology Kharagpur, Kharagpur, India, ³Department of Chemistry, Indian Institute of Technology Bombay, Mumbai, India

OPEN ACCESS

Edited by:

Weijie Yang,
North China Electric Power University,
China

Reviewed by:

Xiaoshuo Liu,
Southeast University, China
Chongchong Wu,
University of Calgary, Canada
Xun-Lei Ding,
North China Electric Power University,
China

*Correspondence:

Pratim Kumar Chattaraj
pkc@chem.iitkgp.ac.in;
0000-0002-5650-7666

Specialty section:

This article was submitted to
Hydrogen Storage and Production,
a section of the journal
Frontiers in Energy Research

Received: 30 September 2021

Accepted: 20 October 2021

Published: 03 November 2021

Citation:

Pal R and Chattaraj PK (2021)
Aromatic Clusters as Potential
Hydrogen Storage Materials.
Front. Energy Res. 9:786967.
doi: 10.3389/fenrg.2021.786967

The scientific community is engrossed in the thought of a probable solution to the future energy crisis keeping in mind a better environment-friendly alternative. Although there are many such alternatives, the green hydrogen energy has occupied most of the brilliant minds due to its abundance and numerous production resources. For the advancement of hydrogen economy, Government agencies are funding pertinent research projects. There is an avalanche of molecular systems which are studied by several chemists for storing atomic and molecular hydrogens. The present review on molecular hydrogen storage focuses on all-metal and nonmetal aromatic clusters. In addition to the effect of aromaticity on hydrogen trapping potential of different molecular moieties, the importance of using the conceptual density functional theory based reactivity descriptors is also highlighted. Investigations from our group have been revealing the fact that several aromatic metal clusters, metal doped nonmetal clusters as well as pure nonmetal clusters can serve as potential molecular hydrogen trapping agents. Reported systems include N_4Li_2 , N_6Ca_2 clusters, Mg_n , and Ca_n ($n = 8-10$) cage-like moieties, $B_{12}N_{12}$ clathrate, transition metal doped ethylene complexes, M_3^+ ($M = Li, Na$) ions, E_3-M_2 ($E = Be, Mg, Al; M = Li, Na, K$) clusters, $Li_3Al_4^-$ ions, Li decorated star-like molecules, B_xLi_y ($x = 3-6; y = 1, 2$), Li-doped annular forms, Li-doped borazine derivatives, $C_{12}N_{12}$ clusters (N_4C_3H) $_6Li_6$ and associated 3-D functional material, cucurbiturils, lithium-phosphorus double-helices. Ni bound $C_{12}N_{12}$ moieties are also reported recently.

Keywords: hydrogen storage, aromaticity, all-metal clusters, nonmetal clusters, conceptual density functional theory

1 INTRODUCTION

With the ever-increasing utilization of energy, whose primary source has been fossil fuels for so long, the rate of carbon dioxide concentration in the atmosphere is increasing at an alarming rate. With this level of energy demand, fossil fuels will soon be exhausted unless more and more clean fuels are adopted. As of 2019, the International Energy Agency (IEA, 2019) reports the world total energy consumption, of which oil source constitutes 40.4%, followed by 19.7% consumption of electricity, 16.4, 10.4, and 9.5% of natural gas, biofuels, and coal, respectively, and 3.6% constitute other sources of energy. Although 2020 has witnessed a significant reduction in global CO_2 emissions (by 2.4 gigatons) and a decline in the usage of electricity owing to the industrial sector shutdown as a part of COVID-19 restrictions, we are far from reaching the goal of saving the world from collapsing due to over usage of non-renewable energy resources. On the bright side, more and more countries are announcing pledges towards attaining net-zero emissions by the year 2050. To achieve such goals,

more and more research projects are being undertaken to search for alternative reliable clean energy sources like hydrogen, nuclear, and efficiently harness the natural resources that we already have in the form of solar, hydro, and wind.

Hydrogen, as a fuel source, is ideal since we have an abundance of it, it causes no emission of harmful gases, and it has a much greater energy content per unit than fossil fuels (World Nuclear Association Website, 2016). The challenges that arise include the conversion of hydrogen from various sources like water and hydrocarbons to its free state, followed by its storage and transportation. The first challenge can be overcome by processes like electrolysis of water and steam reformation of small hydrocarbons, both of which have disadvantages of their own. While the former requires electricity, the latter produces CO₂ as a by-product. Between the two, the electrolysis process seems more preferable since it can be made eco-friendly by using solar, wind, and hydro electricity. Again, there is a downside of higher cost. After the production of free molecular hydrogen, it needs to be stored in an environment with high pressure and very low temperatures. A better way is to adsorb or entrap H₂ in molecular clusters and cages such that the desorption process would also be feasible. Such materials must follow certain standard requirements set by the United States Department of Energy (DOE) (U.S. Department of Energy, USCAR, 2017) to be considered as efficient storage material. In order for a compound to practically act as an effective hydrogen storage material, it must be highly stable, easily available, light weight, inexpensive, showing fast adsorption-desorption kinetics at ambient conditions, can achieve high gravimetric and volumetric hydrogen storage density, and favourable thermodynamic parameters. The appropriate binding energy range depends on the type of hydrogen adsorption on the storage material. For physisorption, it is very small (in the milli-eV range), for chemisorption the value ranges within 2–4 eV, and for the type between physisorption and chemisorption, the binding energy ranges from 0.1 to 0.8 eV. Interaction energy that lies in between that of physisorption and chemisorption is ideal for a better reversible hydrogen storage material.

Hydrogen adsorption can occur via physisorption, chemisorption, and by virtue of Kubas interaction (Kubas, 2001) in the case of transition metals (TM) which is essentially the sequential electron donation from σ_{H} to vacant d_{TM} orbital, and a back donation from filled d_{TM} to σ_{H}^* . The H₂ storage capacity of a diverse range of molecular systems are explored like, nanomaterials based on carbon (Dresselhaus et al., 1999; Froudakis, 2002; Ding et al., 2001; Lochan and Head-Gordon, 2006; Ströbel et al., 2006; Xu et al., 2007), and aluminium nitride (Wang et al., 2009), Li-bound neutral and cationic B_n complexes (Bandaru et al., 2012), alkali-metal doped benzenoid systems (Srinivasu et al., 2009), polyolithiated B N doped graphyne (Jana et al., 2018), clathrate-hydrate molecules (Chattaraj et al., 2011a), Boron-Li clusters (Wu et al., 2008; Yildirim and Güvenç, 2009), transition-metal doped BN systems (Shevlina and Guo, 2006), fullerene clusters (Peng et al., 2009), magnesium clusters (Wagemans et al., 2005), transition-metal coated boron buckyballs, B₈₀ (Wu et al., 2009), and metal-organic frameworks (MOFs) (Rosi et al., 2003; Dinca et al., 2006),

trigonal, aromatic all-metal Li₃⁺ and Na₃⁺ systems as well as alkaline-earth metal (M_n: M = Mg, Ca; n = 8–10) cages (Giri et al., 2011a), transition-metal-ethylene complexes (Chakraborty et al., 2011) and cage-like B₁₂N₁₂ clusters (Giri et al., 2011b).

The aromatic stability of a compound can influence the hydrogen adsorbing power of the molecular motif as described on alkali metal doped hydrocarbons by Srinivasu et al. (2009) Others are discussed in this review. The concept of aromaticity is not yet completely unfolded. It started with being able to explain the reason behind the extra stability in some cyclic hydrocarbons following certain rules prescribed by Hückel, 1931a, Hückel, 1931b, Hückel, 1932. Thorn and Hoffman (1979) then contributed to explaining those of metallabenzene compounds. The accurate measurement of this behaviour is somewhat challenging in the sense that there is no “one-size-fits-all” concept here. Numerous descriptors can measure aromaticity using various techniques but they are highly system-dependent. In this report, we have described the influence of aromatic behaviour on the H₂ trapping potential of various all-metal and nonmetal systems where it is measured in terms of nucleus independent chemical shift (NICS) (Schleyer et al., 1996; Chen et al., 2005) values.

2 COMPUTATIONAL DETAILS

Computational chemistry packages, Gaussian 03 (Frisch et al., 2003) and Gaussian 09 (Frisch et al., 2009), are utilized to model the systems, followed by geometry optimization and frequency calculation. The levels of theory used in this study are MP2, MPW1K, M05-2X, M06, B3LYP, B3LYP-D3, ω B97X-D, and PBE0, with basis sets like 6-31G, 6-31+G(d), 6-311+G(d), 6-311+G(d,p), cc-pVDZ, and Def2-TZVP. The aromaticity is evaluated in terms of NICS values (Chen et al., 2005) at various distances from the molecular plane. Global and local reactivity descriptors like electronegativity (χ) (Parr et al., 1978), chemical hardness (η) (Parr and Pearson, 1983; Pearson, 1997) and electrophilicity index (ω) (Parr et al., 1999; Chattaraj and Roy, 2007; Chattaraj et al., 2011b) Fukui functions (f_{r}^{\pm}) (Parr and Yang, 1984), atomic charges (q_{k}), and philicity (ω_{k}^{\pm}) (Chattaraj et al., 2003) derived from the Conceptual density functional theory (CDFT) help describe the molecular stability and reactivity. Following equations are followed for the calculation of the aforementioned descriptors:

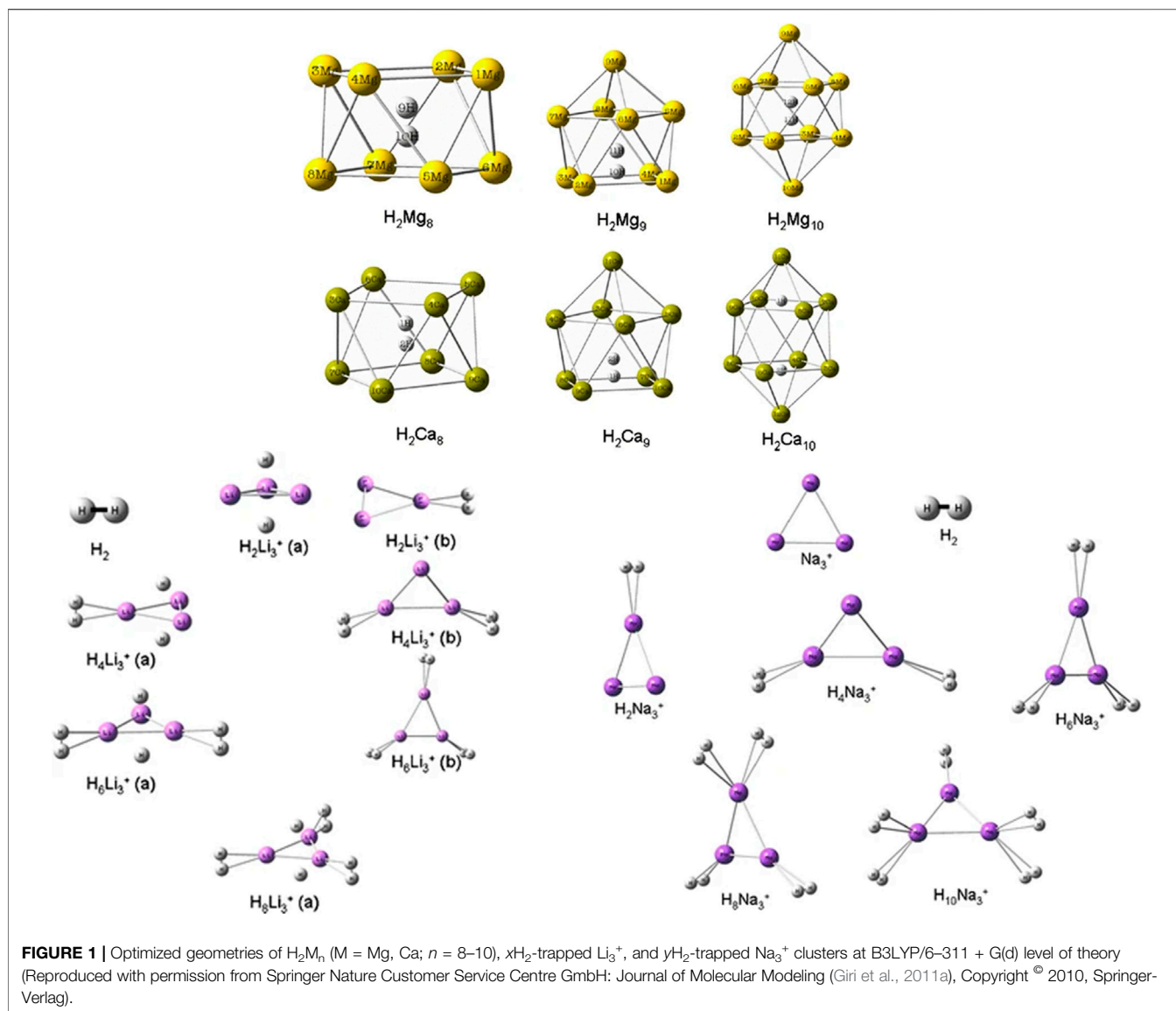
$$\mu = \left(\frac{\partial E}{\partial N} \right)_{v(r)} = -\chi \quad (1)$$

$$\mu = -\chi \approx -\frac{IP + EA}{2} \approx \frac{\epsilon_{\text{HOMO}} + \epsilon_{\text{LUMO}}}{2} \quad (2)$$

$$\eta = \left(\frac{\partial \mu}{\partial N} \right)_{v(r)} = \left(\frac{\partial^2 E}{\partial N^2} \right)_{v(r)} \approx IP - EA \quad (3)$$

$$\omega = \frac{\mu^2}{2\eta} = \frac{\chi^2}{2\eta} \quad (4)$$

$$f(r) = \left(\frac{\delta \mu}{\delta v(r)} \right)_N = \left(\frac{\partial \rho(r)}{\partial N} \right)_{v(r)} \quad (5)$$



$$f_k^- = \left(\frac{\partial \rho}{\partial N} \right)_{v(r)}^- \cong p_k(N) - p_k(N-1) [\text{for electrophilic attack}] \quad (6a)$$

$$f_k^+ = \left(\frac{\partial \rho}{\partial N} \right)_{v(r)}^+ \cong p_k(N+1) - p_k(N) [\text{for nucleophilic attack}] \quad (6b)$$

$$f_k^0 = \left(\frac{\partial \rho}{\partial N} \right)_{v(r)}^0 \cong \frac{1}{2} (p_k(N+1) - p_k(N-1)) [\text{for radical attack}] \quad (6c)$$

$$\omega_k^\alpha = \omega \cdot f_k^\alpha \quad (7)$$

where E stands for total energy and N for a total number of electrons in the system, ϵ_{HOMO} , ϵ_{LUMO} , IP, and EA refer to highest occupied and lowest unoccupied molecular orbital energies, ionization potential, and electron affinity,

respectively. μ denotes chemical potential (Parr and Yang, 1989), $\rho(r)$ denotes electron density, p_k stands for the electron population at the k th atomic site, and α can be 0, +, or -, for radical, nucleophilic, and electrophilic attacks, respectively.

3 CASE STUDIES

3.1 ALL-METAL Clusters

3.1.1 Mg/Ca_n and Li/Na₃⁺ Clusters

The hydrogen storage potential of magnesium and calcium cages (Mg_n and Ca_n ; $n = 8-10$) along with that of trigonal alkali-metal cationic clusters (Li_3^+ and Na_3^+) were explored by Giri et al. (2011a) with a CDFT approach. The stability of $1H_2$ -trapped Mg_n and Ca_n complexes increases with increase in n . It is, however, interesting to discover that these bare cages could not be

TABLE 1 | Reaction energy in kcal/mol for the gradual hydrogen loading on Li_3^+ and Na_3^+ clusters (Adapted with permission from Springer Nature Customer Service Centre GmbH: Journal of Molecular Modeling (Giri et al., 2011a), Copyright © 2010, Springer-Verlag).

Reaction	ΔE
$\text{Li}_3^+ + \text{H}_2 = \text{H}_2\text{Li}_3^+ \text{ (a)}$	-32.188
$\text{H}_2\text{Li}^+ \text{ (a)} + \text{H}_2 = \text{H}_4\text{Li}_3^+ \text{ (a)}$	-3.677
$\text{H}_4\text{Li}_3^+ \text{ (a)} + \text{H}_2 = \text{H}_6\text{Li}_3^+ \text{ (a)}$	-3.631
$\text{H}_6\text{Li}_3^+ \text{ (a)} + \text{H}_2 = \text{H}_8\text{Li}_3^+ \text{ (a)}$	-3.584
$\text{Li}_3^+ + \text{H}_2 = \text{H}_2\text{Li}_3^+ \text{ (b)}$	-2.508
$\text{H}_2\text{-Li}_3^+ \text{ (b)} + \text{H}_2 = \text{H}_4\text{Li}_3^+ \text{ (b)}$	-2.346
$\text{H}_4\text{-Li}_3^+ \text{ (b)} + \text{H}_2 = \text{H}_6\text{Li}_3^+ \text{ (b)}$	-2.168
$\text{Na}_3^+ + \text{H}_2 = \text{H}_2\text{Na}_3^+$	-0.697
$\text{H}_2\text{-Na}_3^+ + \text{H}_2 = \text{H}_4\text{Na}_3^+$	-0.639
$\text{H}_4\text{-Na}_3^+ + \text{H}_2 = \text{H}_6\text{Na}_3^+$	-0.569
$\text{H}_6\text{-Na}_3^+ + \text{H}_2 = \text{H}_8\text{Na}_3^+$	-0.200
$\text{H}_8\text{-Na}_3^+ + \text{H}_2 = \text{H}_{10}\text{Na}_3^+$	-0.165

stabilized *i.e.*, before trapping the H_2 molecule within them. Again, in the cases of H_2 -bound Li_3^+ and Na_3^+ systems, the stability is found to increase with the increase in the number of bound H_2 molecules. Upon binding with the clusters, most of the H_2 retains their molecular identity, except in a few of the $n\text{H}_2\text{Li}_3^+$ systems where one of the H_2 molecules dissociates and binds itself in the atomic form. This behaviour is also observed in the case of H_2 -trapped Ca_{10} cage (Figure 1). The planarity of the Li_3^+ and Na_3^+ clusters remained intact in the H_2 -bound complexes. Further analysis of the changes in the CDFT based reactivity indices, *viz.*, electronegativity (χ) hardness (η) and electrophilicity (ω), revealed a gradual decrease in the ω values with an increase in the number of H_2 molecules.

The NICS (0, 1) values calculated for the top and bottom M_4 rings ($M = \text{Mg}, \text{Ca}$) of the H_2 -encapsulated Mg_n and Ca_n cages are found to be negative, indicating the existence of diatropic ring current at the said positions. Similarly, negative NICS_{zz} (0) values for the poly-hydrogenated trigonal clusters also established the aromatic stability with gradual H_2 uptake. Further, from a thermodynamic point of view, the negative values of the reaction energy (ΔE_b , kcal/mol) for the sequential H_2 binding on the Li_3^+ and Na_3^+ systems provide some theoretical justification towards their possible usage as hydrogen storage materials (Table 1).

3.1.2 Be_3M_2 , Mg_3M_2 , and Al_4M_2 ($M = \text{Li}, \text{Na}, \text{K}$) Clusters

The aromaticity of all-metal Al_4^{2-} system was previously reported (both theoretically and experimentally) (Li et al., 2001), followed by that of Be_3^{2-} and Mg_3^{2-} systems (Kuznetsov and Boldyrev, 2004; Roy and Chattaraj, 2008; Giri et al., 2010). All these systems owe their aromatic behaviour to the presence of delocalized π -electrons. The motivation for using these systems with the alkali metal counterion M^+ ($M = \text{Li}, \text{Na}$, and K) (Srinivasu et al., 2012) is backed by the logic that due to high polarization, the M centers will be highly electropositive and hence can serve as a suitable site for hydrogen adsorption. The optimized geometries of the systems under study are provided in Figure 2, and their hydrogen adsorbed structures are depicted in Figure 3. The

positive charges carried by the M centers were found to be proportional to the difference in electronegativity values between the two types of metal species in the complex. This difference is lower in Mg_3M_2 as compared to that in Be_3M_2 and Al_4M_2 , which causes a lower charge transfer from M to the Mg_3 ring compared to the others. This, in turn, results in poor H_2 adsorption in the Mg_3M_2 complexes (interaction energy of -0.5 kcal/mol per H_2 , compared to the same ranging between -1.8 to -3.1 and -2.7 to -3.2 kcal/mol per H_2 for Be_3M_2 and Al_4M_2 , respectively). Now, from the perspective of the alkali metals, a high ionic radius and low charge density (*i.e.*, low ionic potential) on the potassium atom results in a very weak interaction with the K atom containing systems (as low as -0.6 kcal/mol per H_2). Both Be_3Li_2 and Be_3Na_2 are found to adsorb six hydrogen molecules each (three per alkali metal atom), whereas Al_4Li_2 and Al_4Na_2 are capable of binding eight molecules each (four H_2 per alkali metal atom). The gravimetric weight percentage of hydrogen adsorption for the

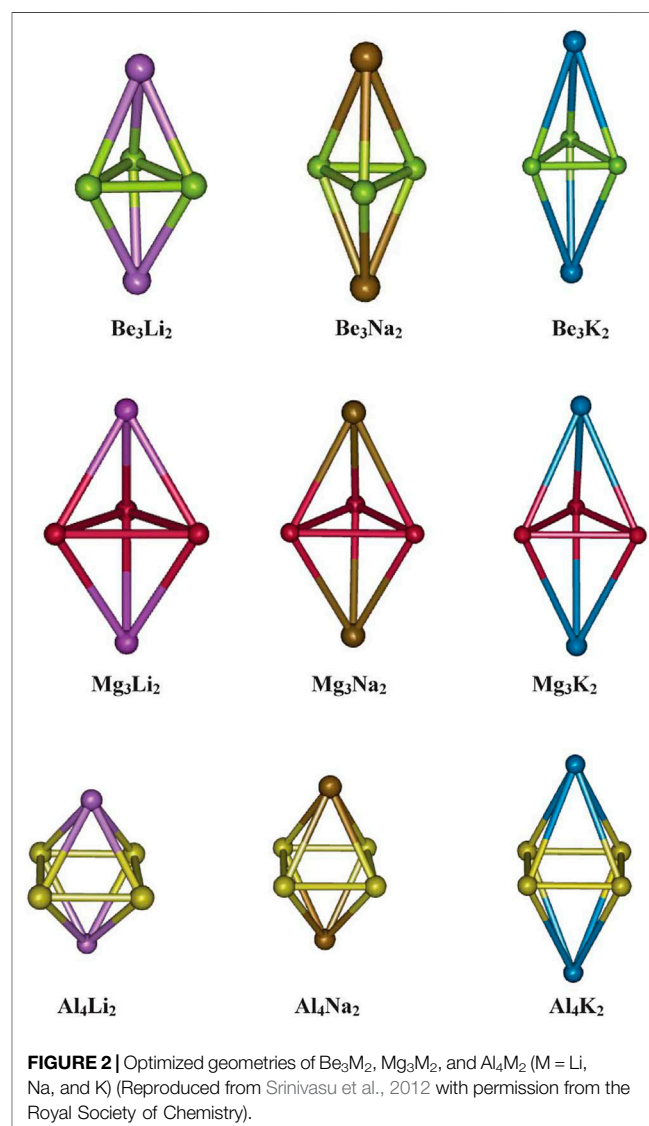
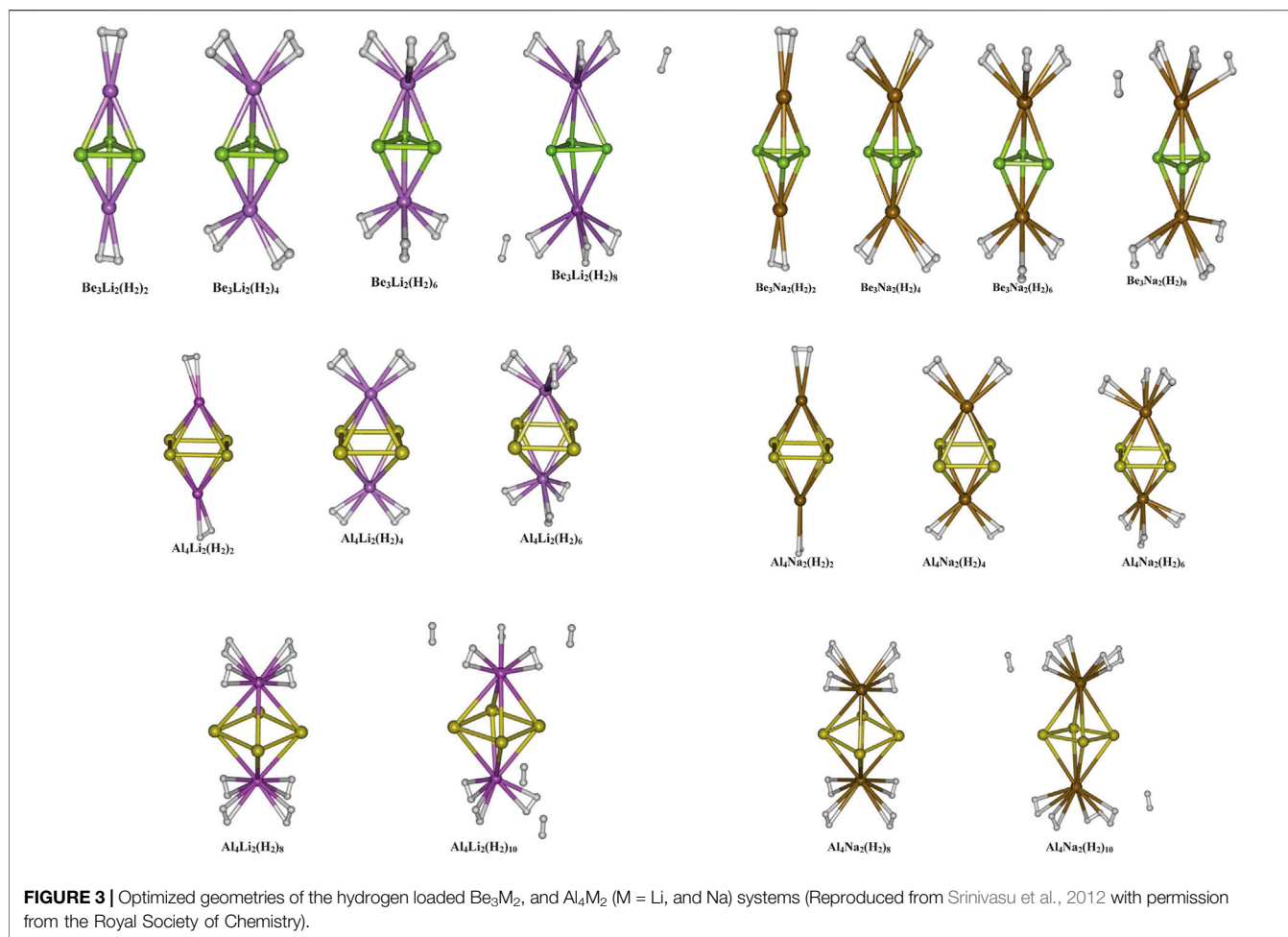


FIGURE 2 | Optimized geometries of Be_3M_2 , Mg_3M_2 , and Al_4M_2 ($M = \text{Li}, \text{Na}$, and K) (Reproduced from Srinivasu et al., 2012 with permission from the Royal Society of Chemistry).



former two are 22.64 and 14.12, those for Al_4Li_2 and Al_4Na_2 are 11.59 and 9.4, respectively. Evidently, Be_3Li_2 is preferred to Al_4Li_2 in terms of the gravimetric density, whereas with respect to the binding energy per H_2 molecule, Al_4Li_2 is preferred as a better hydrogen storage material.

The stability of these hydrogenated systems is established in terms of higher energy gaps (5.17–6.40 eV) between their respective HOMO and LUMO. The variation in total energy (E), χ , η , and ω also serve as good descriptors for judging the reactivity and stability of the molecular species. A uniform decrease in E , and decrease in ω values with increasing H_2 adsorption describes the stabilization of the metal clusters upon hydrogenation. η also shows a gradual increase in most of the cases. The aromaticity of Be_3M_2 and its hydrogenated species calculated in terms of NICS values at 0, 0.5, and 1 are highly negative and show very low variation with the number of H_2 molecules loaded. For the Al_4M_2 cluster, however, most of the NICS values are found to be positive, even though it is an established fact that the Al_4^{2-} species has aromatic stability. The variation of aromaticity with the number of adsorbed H_2 molecule is also found to be quite random and significantly high. Clearly, NICS is not a good indicator for the Al_4M_2 clusters.

3.2 NON-METALLIC Aromatic Clusters

3.2.1 Planar Molecular Stars

Several non-metallic aromatic/anti-aromatic clusters are also explored to understand the influence of aromaticity on their hydrogen adsorbing or trapping potential. Replacing the H atoms from planar hydrocarbon rings like C_4H_4 , C_5H_5^- , and C_6H_6 with Li atoms results in the formation of star-shaped molecular clusters since the Li atoms prefer to bind two adjacent C atoms *via* a bridging bond (**Figure 4**) (Giri et al., 2011c). The partial positive charges on the Li centers enable them to readily adsorb H_2 molecules. Each Li atom in C_5Li_5^- can efficiently bind with only one H_2 (binding energy of -2.1 kcal/mol per H_2), whereas those in the neutral clusters (*i.e.*, in C_4Li_4 and C_6Li_6) can bind up to two H_2 molecules with binding energies ranging within -2.5 to -3.3 kcal/mol per H_2 . A thorough analysis of the NICS-scan (0–5 Å) plots (**Figure 5**) for each of the studied species provides useful information regarding the variation in the degree of aromaticity/anti-aromaticity with gradual hydrogen loading. The antiaromatic nature of C_4H_4 is found to be enhanced in its lithium analogue. It further increases in the $4\text{H}_2@C_4\text{Li}_4$ system, followed by a decrease in $8\text{H}_2@C_4\text{Li}_4$ where the NICS (0) value falls below those of the parent moieties

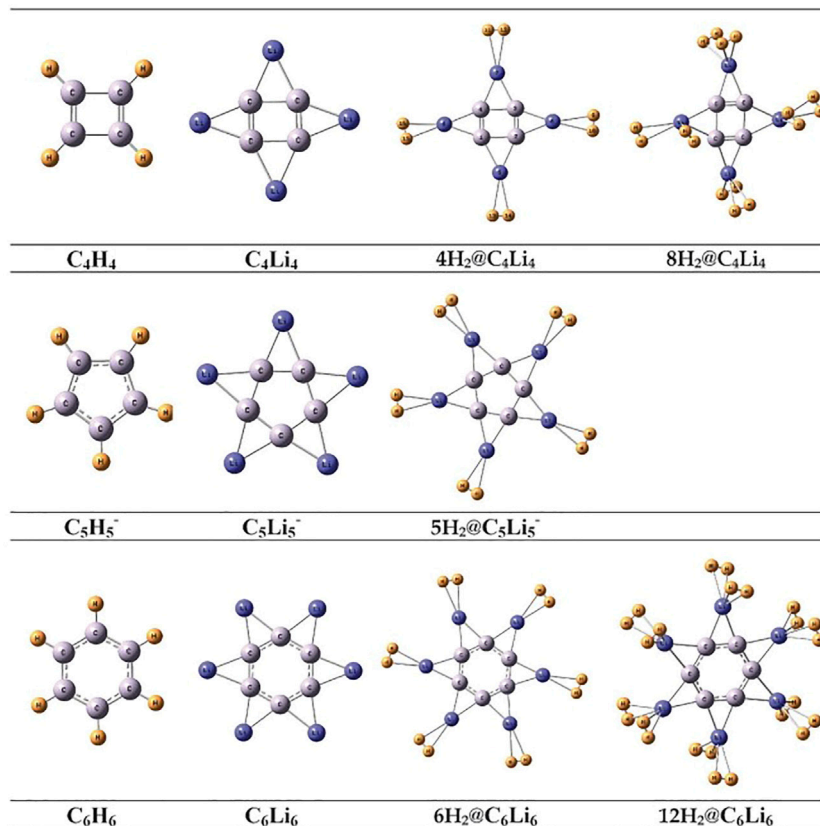


FIGURE 4 | Optimized geometries of C_nH_n ($n = 4-6$), their Li analogues, and H_2 trapped C_nLi_n ($n = 4-6$) systems at B3LYP/6-311+G (d,p) level of theory (Reproduced from Giri et al., 2011c with permission from the PCCP Owner Societies).

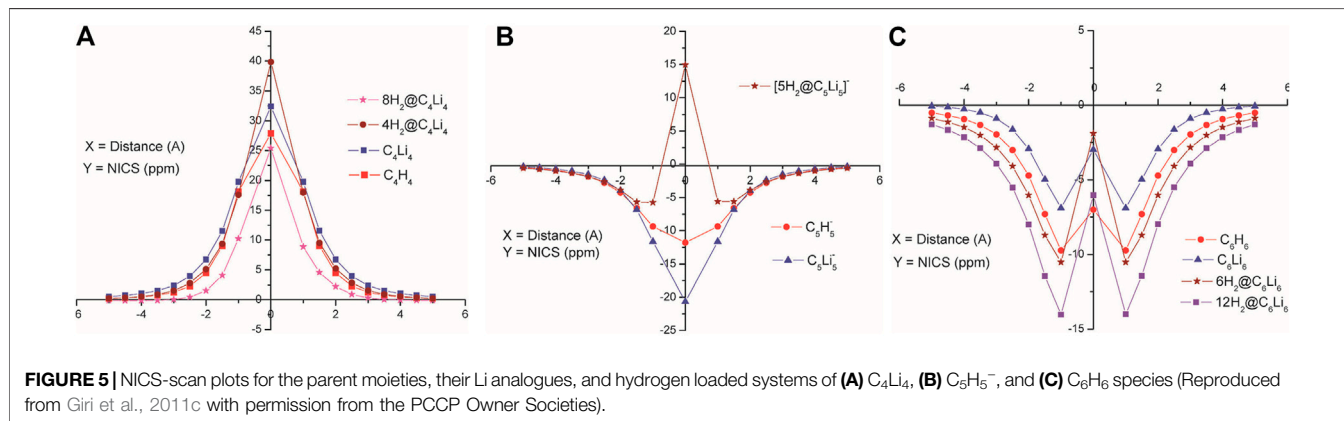
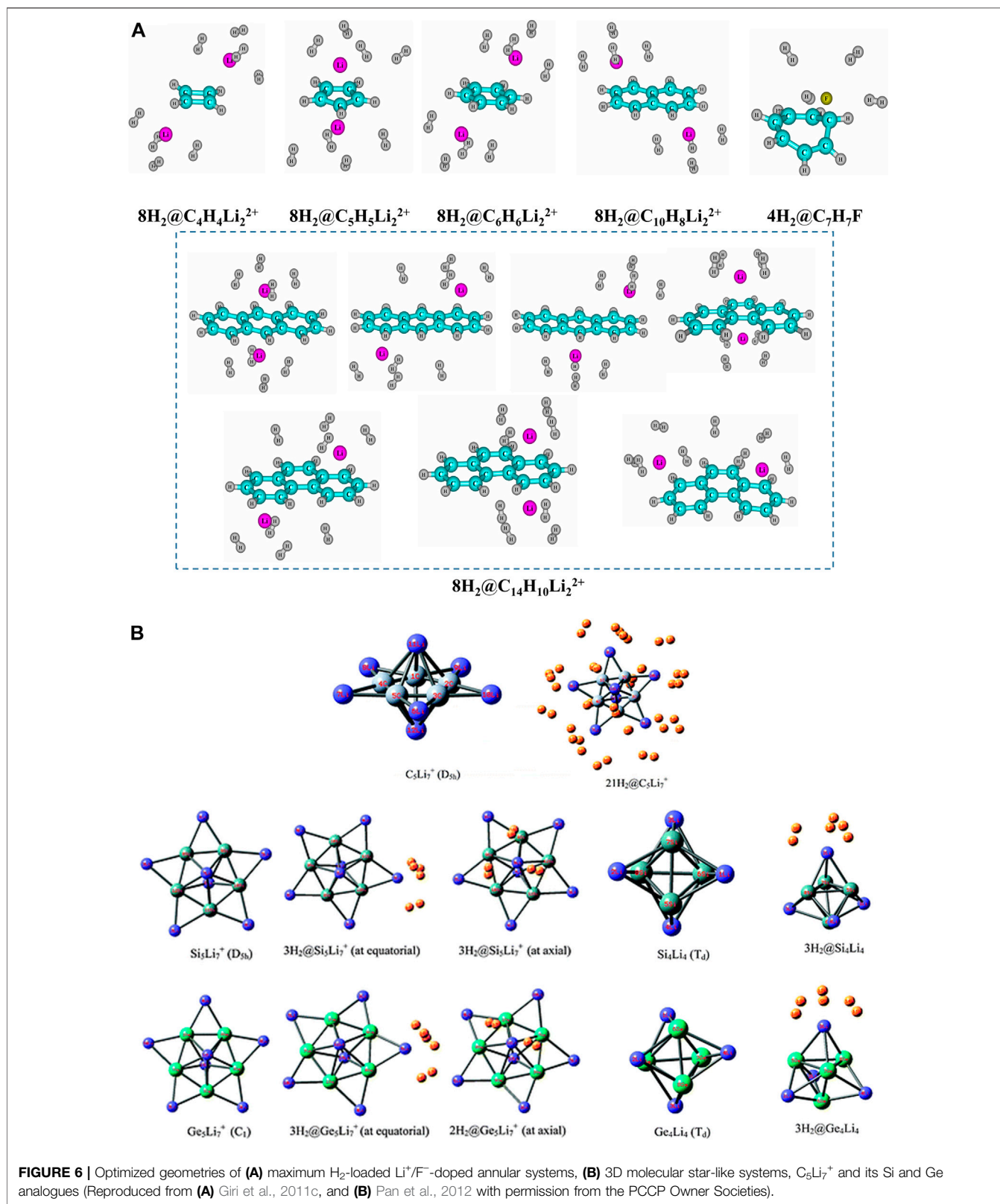


FIGURE 5 | NICS-scan plots for the parent moieties, their Li analogues, and hydrogen loaded systems of (A) C_4Li_4 , (B) $C_5H_5^-$, and (C) C_6H_6 species (Reproduced from Giri et al., 2011c with permission from the PCCP Owner Societies).

(Figure 5A). Since the C_4Li_4 species is more likely to exist in the $8H_2$ -bound form, it can be arguably stated that hydrogen adsorption on C_4Li_4 reduces its antiaromatic nature, which is favourable in terms of explaining the stability of these clusters. In the case of the aromatic $C_5H_5^-$ ring, lithiation increases its aromatic nature as evident from Figure 5B. The $5H_2$ -bound $C_5Li_5^-$ complex follows the same trend as the parent moieties

while moving from NICS (4) to NICS (1), *i.e.*, they gradually decrease with decreasing distance from the ring center. However, unlike the parent moieties, $5H_2@C_5Li_5^-$ shows an unexpected rise in NICS (0) value rendering it anti-aromatic. Again, unlike in C_5 -species, the aromaticity reduces in the lithium analogue of C_6H_6 complex. Although all the species maintain their aromatic behaviour, the degree of aromaticity



initially decreases with hydrogen loading (*i.e.*, in $6\text{H}_2@C_6\text{H}_6$) with a final increase in the $12\text{H}_2@C_6\text{H}_6$ species (**Figure 5C**). These plots provide ample evidence regarding the dominant

π -ring current in the C_6 species compared to that in the C_5 complexes, which results in an enhanced H_2 -trapping ability in the former.

3.2.2 Li-Doped Annular Systems and 3D Molecular Stars

The H_2 binding ability of a series of lithium ion complexed hydrocarbons (Li^+ above and below the planar ring), *viz.*, C_6H_6 , $C_{10}H_8$, and $C_{14}H_{10}$ are explored in the same study (Giri *et al.*, 2011c), along with that of an F^- ion stabilized tropylium complex. Each Li atom in these systems can store up to four H_2 molecules (**Figure 6A**). The same is true for the C_7H_7F system, even though, unlike the Li^+ -complexed hydrocarbons, $C_7H_7^+$ loses its planarity and hence aromaticity on complexation with F^- . Other 3D molecular star-like systems like $C_5Li_7^+$ (π -aromatic and σ -nonaromatic) and its Si analogue (σ - and π -aromatic) can bind up to a maximum of 21 H_2 molecules (three per Li center) with a gravimetric wt% of 28.0 and 18.3, respectively (Pan *et al.*, 2012; Perez-peralta *et al.*, 2011; Tiznado *et al.*, 2009) (**Figure 6B**). The Ge analogue has a maximum capacity of 19 H_2 molecules with 9.3 wt% of H_2 (Contreras *et al.*, 2013). It is a well-known fact that temperature and pressure can act as tuning parameters in various adsorption/desorption processes. An interesting study performed on a series of Li clusters (BLi_6^+ , $O_2Li_5^+$, $N_2Li_7^+$, $B_2Li_{11}^+$, OLi_3^+ , $C_2Li_9^+$, $F_2Li_3^+$, and FLi_2^+) was reported by Pan *et al.* (2012) where they have achieved enhanced interaction between Li and H_2 by applying an external electric field. By gradually varying the field in the range 0.001–0.005 au, the negative ΔE value increases indicating improved interaction.

3.2.3 Lithium Doped Boron Hydrides

A discussion on hydrogen storage warrants the inclusion of boron hydrides. Metal borohydrides like $LiBH_4$ and $NaBH_4$ are reported to be good hydrogen storage materials (Kojima *et al.*, 2002; Züttel *et al.*, 2003; Liang *et al.*, 2010). The effect of aromaticity on the structural preference of both neutral and ionic boron hydrides with the general formula B_3H_n ($n = 3-9$) was reported by Korkin *et al.* (1995). A similar study (Bandaru *et al.*, 2012) was performed on several boron-lithium complexes with the general formula B_xLi_y ($x = 2-6$; $y = 1, 2$) where the cationic species show a higher H_2 binding capacity than their neutral counterparts owing to the greater net positive charge on the Li centers in the former. Among various boron hydrides, $B_3H_3^{2-}$ can be considered as the iso-electronic boron-analogue of the aromatic cyclopropenium ion (Garratt, 1986; Minkin *et al.*, 1994). A theoretical study on $B_3H_3^{2-}$ and its various Li doped species performed by Pan *et al.* (2011) investigates the H_2 storage process *via* an interaction that lies somewhere between physisorption and chemisorption. The aromaticity of these systems is evident from the negative values of NICS (0) (ranging within -3.32 – -29.38) and NICS (1) (varies from -7.48 to -17.91). The parent moiety itself is capable of adsorbing a maximum of 11 H_2 molecules. Here, the importance of the dispersion interaction is clearly reflected from the interaction energy values obtained before and after including the dispersion corrected terms in the theoretical calculations. For example, the interaction energy per H_2 molecule in the maximum H_2 -loaded systems ranges within -1.2 – -1.9 kcal/mol, which changes to a range of

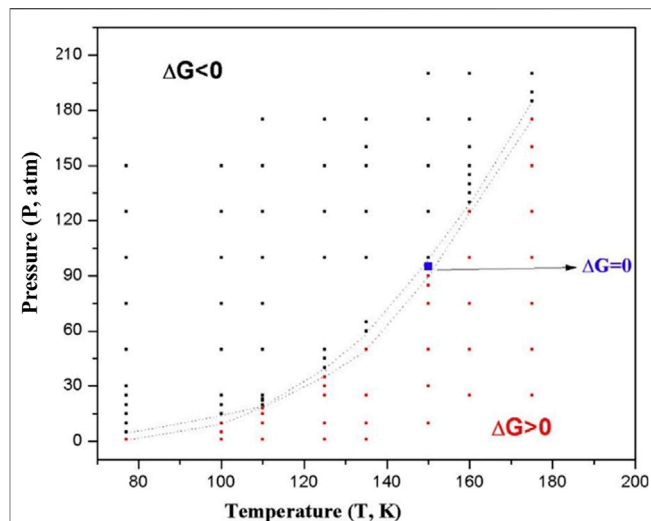


FIGURE 7 | T-P phase diagram for the adsorption of six H_2 molecules on $B_3(\mu-Li)_3H_3^+$. The black markers indicate regions of favourable adsorption and red markers indicate that of favourable desorption (Reproduced from Pan *et al.*, 2011 with permission from John Wiley and Sons. Copyright © 2011 Wiley Periodicals, Inc.).

-2.6 – -5.6 kcal/mol after dispersion correction. Although judging by parameters like the H_2 binding capacity, and gravimetric wt% of H_2 , the $B_3H_3^{2-}$ system seems to be a preferable choice, it is yet to be experimentally realized. In that regard, $B_3(\mu-Li)_3H_3^+$ species is a better alternative with high aromatic stability. The H_2 molecules are mostly bound by weak interaction and most of the adsorption process shown here is endergonic in nature. Thus an optimal condition for these processes to be feasible would be that of high pressure (P) and low temperature (T). A T-P phase diagram (**Figure 7**) for the adsorption of 6 H_2 molecules on $B_3(\mu-Li)_3H_3^+$ depicts the variation of free energy change with the change in T and P, where black markers indicate regions of favourable adsorption and red markers indicate that of favourable desorption.

3.2.4 Planar N_4^{2-} and N_6^{4-} Rings

A study (Duley *et al.*, 2011) reported on the aromaticity and hydrogen storage in the inorganic analogues of cyclobutadiene and benzene rings, *i.e.*, N_4^{2-} and N_6^{4-} reveals the anti-aromatic and aromatic natures, respectively. The NICS-scan plots of all four systems are provided in **Figure 8** where it can be clearly seen that the NICS variation of N_6^{2-} follows a similar trend as that of the benzene, whereas this is not the case for N_4^{2-} and cyclobutadiene. The otherwise antiaromatic N_4^{2-} ring shows aromaticity at a distance of 1 Å above the molecular plane, and gradually decreases away from the ring. Thus, a positive NICS (0) value and a negative NICS (1) value makes it σ -antiaromatic and π -aromatic. These anionic clusters are stabilized by complexation with lithium and calcium counterions to form N_4Li_2 and N_6Ca_2 (optimized structures provided in **Figure 9**). Each Li center is found to bind with

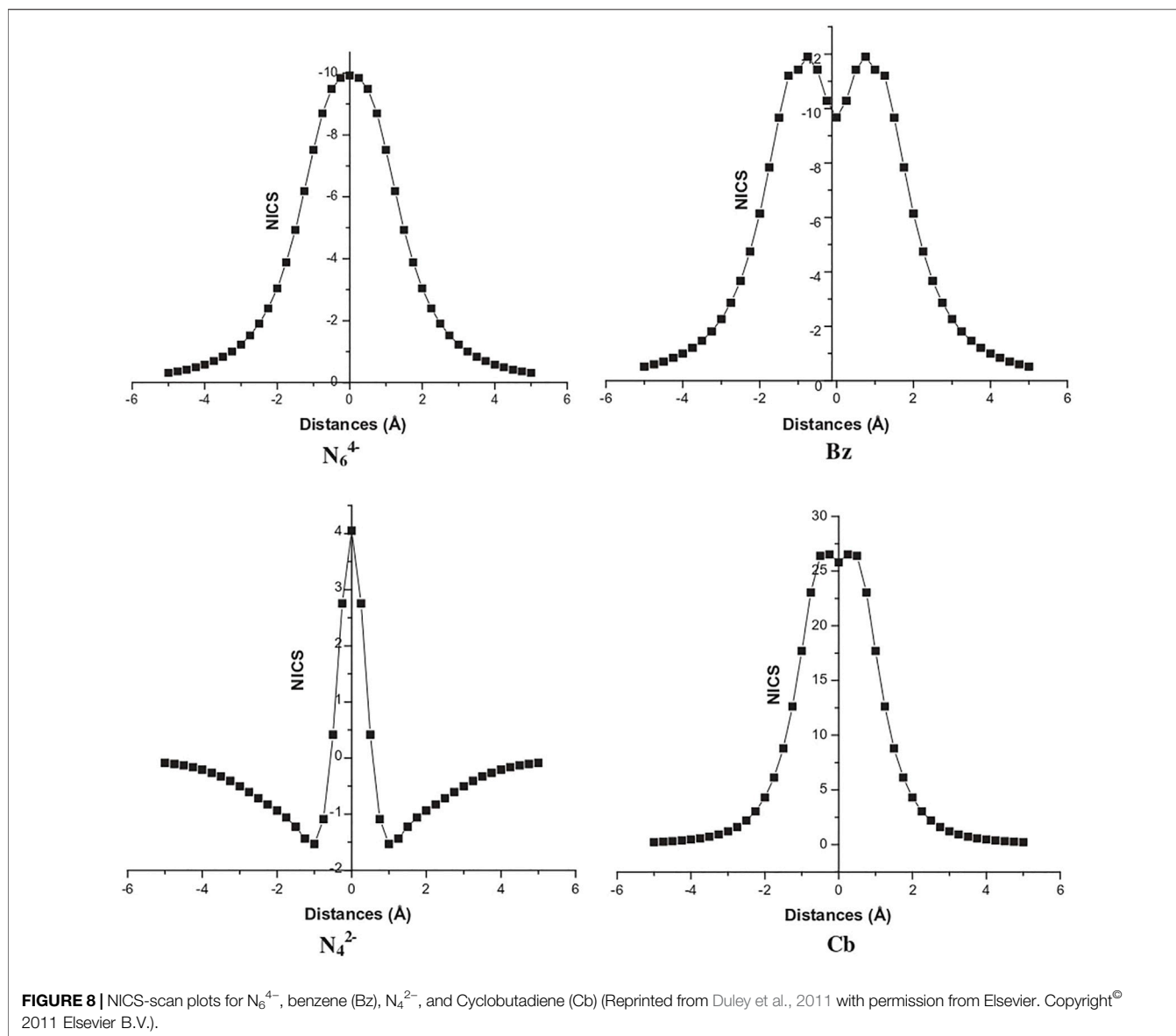


FIGURE 8 | NICS-scan plots for N_6^{4-} , benzene (Bz), N_4^{2-} , and Cyclobutadiene (Cb) (Reprinted from Duley et al., 2011 with permission from Elsevier. Copyright© 2011 Elsevier B.V.).

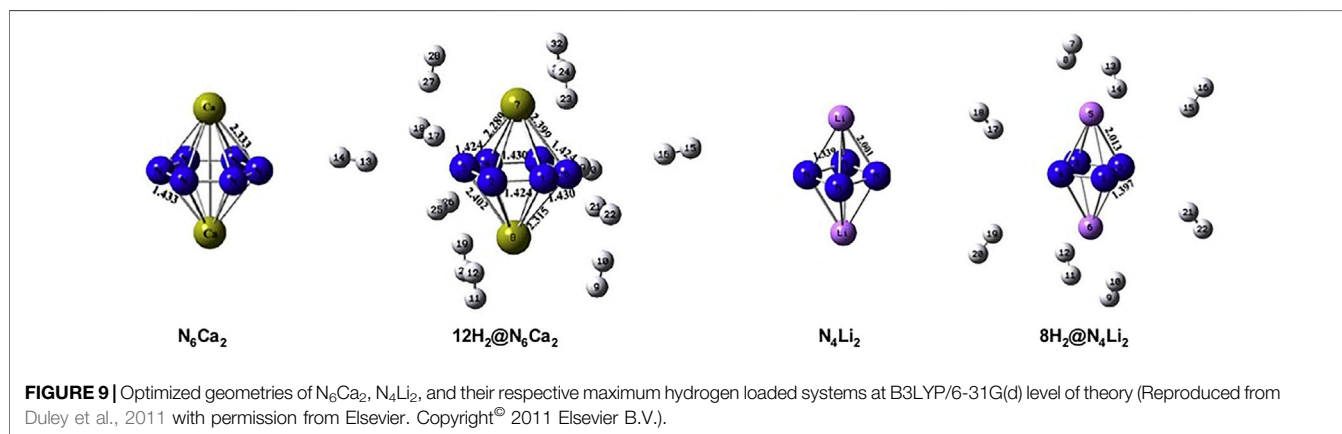


FIGURE 9 | Optimized geometries of N_6Ca_2 , N_4Li_2 , and their respective maximum hydrogen loaded systems at B3LYP/6-31G(d) level of theory (Reproduced from Duley et al., 2011 with permission from Elsevier. Copyright© 2011 Elsevier B.V.).

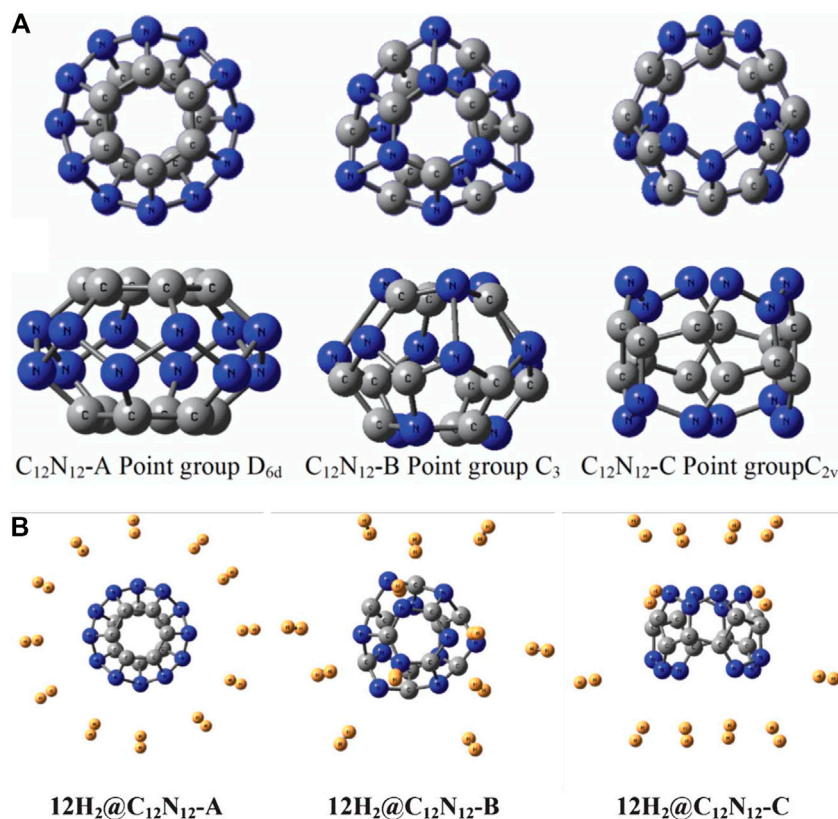


FIGURE 10 | The optimized geometries of **(A)** the three isomers of $C_{12}N_{12}$ cage (**top and side view**), and **(B)** their respective 12 H_2 loaded structures at B3LYP-D3/6-31G(d) level of theory (Reproduced from Mondal et al., 2013 with permission from the Royal Society of Chemistry).

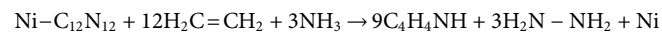
up to four H_2 ($\Delta E = -1.2$ kcal/mol) and each Ca center adsorbs up to six H_2 molecules ($\Delta E = -1.3$ kcal/mol).

3.2.5 $C_{12}N_{12}$, $B_{12}N_{12}$, and Ni-Decorated $C_{12}N_{12}$ Cages

$C_{12}N_{12}$ cage can have three possible isomers, viz., $C_{12}N_{12}$ -A, $C_{12}N_{12}$ -B, and $C_{12}N_{12}$ -C with the optimized structures having D_{6d} , C_3 , and C_2 point group symmetries, respectively (**Figure 10A**) (Mondal et al., 2013). Unlike isomers A and B, C is an open cage structure and hence is the most stable of the lot. Although the NICS (0) for all the isomers are found to be negative, isomers A and B do not obey the Spherical Aromaticity rule [$2(N+1)^2$ π -electrons], and isomer C does not follow the Open-Shell Spherical Aromaticity rule [$(2N^2 + 2N + 1)$ π -electrons]. Although, the hydrogen may be expected to bind at three possible sites: N, C, and bridging C and N, the minimum energy structures are obtained only for the N-site adsorption. All the isomers are capable to bind 12 H_2 molecules providing a gravimetric wt% of 7.2 (**Figure 10B**). These clusters can have potential applications as high energy density materials (HEDMs) since they have high heat of formation values (ΔH_f^0). These ΔH_f^0 values (1747.759, 1758.442, and 1813.864 kcal/mol for isomers A, B, and C, respectively) are calculated using the following isodesmic reaction:

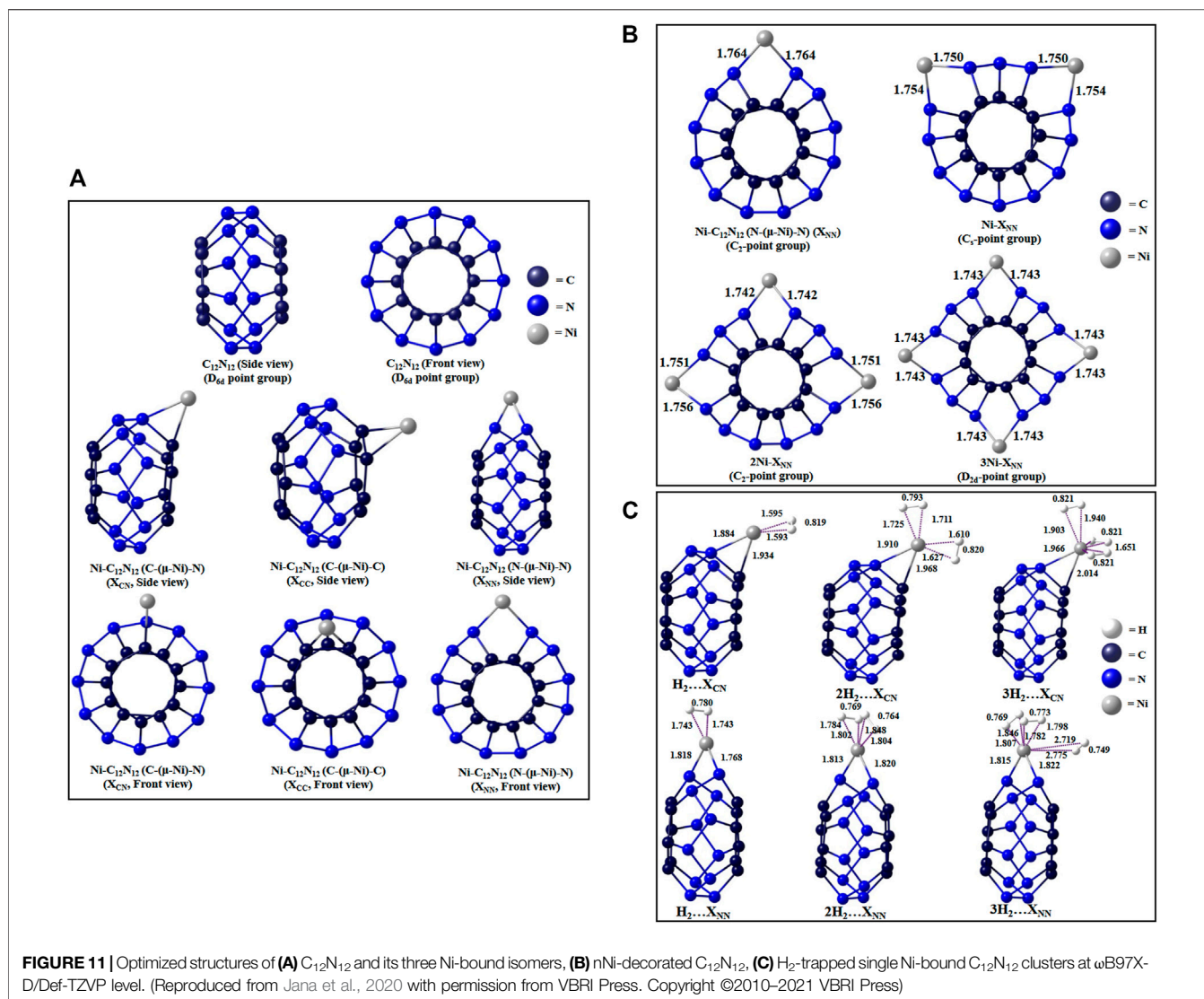


The Ni-decorated analogue (Jana et al., 2020) of the cage can have three possible binding modes: bridging between C and N (denoted as X_{CN} isomer), between 2 C atoms (X_{CC} isomer), or between 2 N atoms (X_{NN} isomer) (**Figure 11A**). Higher numbers of Ni decoration (up to four) in the N-(μ -Ni)-N bridging mode reveals the variation in aromaticity and H_2 -binding potential with the number of Ni atoms (**Figure 11B**). The reason for selecting N-(μ -Ni)-N bridging mode for this purpose is the highest amount of positive charge on the Ni center of the X_{NN} isomer. The isodesmic reactions used to determine the ΔH_f^0 of Ni- $C_{12}N_{12}$ (4,239.470 kcal/mol) and 4Ni- $C_{12}N_{12}$ (4,520.528 kcal/mol) are as follows:



Each Ni center on $C_{12}N_{12}$ is capable to adsorb up to three H_2 molecules (**Figure 11C**). In the single Ni-doped clusters, the aromaticity increases in the order $X_{CN} < X_{CC} < X_{NN}$, and in the case of multiple Ni-doping, the aromaticity increases uniformly with the number of Ni atoms.

The boron analogue of the $C_{12}N_{12}$ cage, i.e., $B_{12}N_{12}$ can trap hydrogen both endohedrally and exohedrally (Giri et al., 2011b). A total of 12 hydrogen molecules can be adsorbed in this cage system, the interaction energy per H_2 molecule



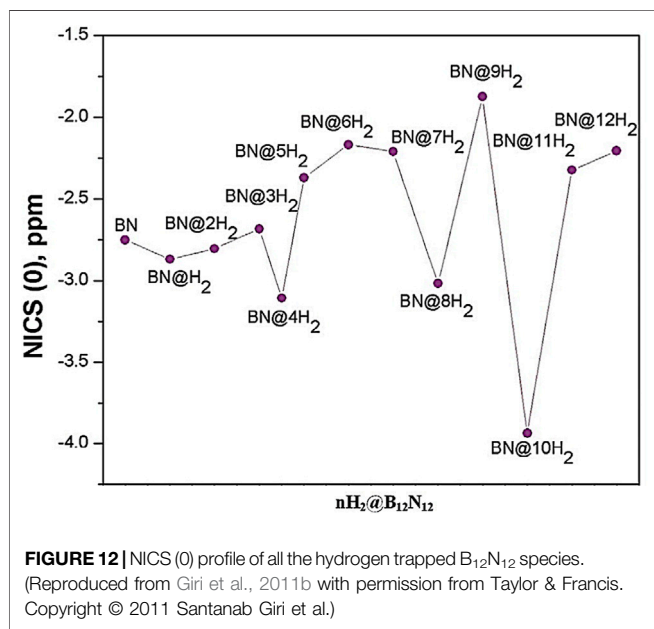
varies from -11.5 to -12 kcal/mol. The change in the reactivity descriptors with the gradual hydrogen uptake validates the CDFT based electronic structure principles. The aromaticity in terms of NICS (0) values of all the $nH_2@B_{12}N_{12}$ ($n = 0-12$) species are plotted and presented in **Figure 12**. It is evident that among all the hydrogen-loaded species, the four, eight, and twelve numbers of H_2 loaded clusters have high aromatic stability.

In this report, we have described the influence of aromatic behaviour on the H_2 trapping potential of various all-metal and nonmetal systems where it is measured in terms of nucleus independent chemical shift (NICS) values. The effect of aromaticity is not uniform throughout all systems. In some systems, the variation of aromaticity with the number of adsorbed H_2 molecule is quite uniform and systemic, like in the cases of C_4Li_4 , $C_5Li_5^-$, and C_6Li_6 rings, N_4^{2-} and N_6^{4-} rings, the nNi -decorated $C_{12}N_{12}$

clusters. While for others, like that in the Al_4M_2 clusters, it is found to be quite random and significantly high. It deserves a careful scrutiny.

4 CONCLUSION

In this review, we have covered several case studies predicting all-metal and non-metal aromatic clusters with potential applications in hydrogen storage and highlighted the effect of aromaticity on the hydrogen uptake potential. The aromatic stabilization present in these clusters enables them to be applicable as promising building blocks for nanomaterials. The NICS-scan plots turn out to be very helpful in understanding the degree and trend in the variation of the aromatic/anti-aromatic nature. The presence of an electropositive center in the molecular clusters provides a



suitable site for the H_2 molecules to undergo a dipole-induced dipole interaction for adsorption. Temperature and pressure are good tuning parameters in controlling the adsorption/desorption process. In this context, a T-P phase diagram can provide proper guidance as to which temperature and pressure range could be ideal to undergo a favourable adsorption process. We have also highlighted the use of external electric field in tuning the H_2 loading and release processes and hence overall improving the H_2 trapping capacity of the cluster in question. For future research, the search for chemical frameworks with

large surface area and high porosity can be made for better reversible hydrogen storage *via* physisorption having interaction energy closer to that of chemisorption, with a target of improving the gravimetric and volumetric storage capacity, favourable rates of adsorption and desorption, operating temperatures, and thermal conductivity. Molecular frameworks offering higher surface area to volume ratio can increase volumetric capacity. The binding energies can be increased by tuning the pore volume, and the thermal conductivity can be improved with the help of new and developed heat exchangers.

AUTHOR CONTRIBUTIONS

PC came up with the concept and design of the review, wrote the abstract, reviewed the final manuscript. RP contributed towards the literature survey, writing the manuscript. All authors contributed to manuscript revision, read, and approved the submitted version.

ACKNOWLEDGMENTS

PC would like to thank Dr. Weijie Yang for kindly inviting him to contribute an article to the research topic “Computational Design of Advanced Materials for Hydrogen Storage and Production” in the journal, *Frontiers in Energy Research*. He also thanks DST, New Delhi, for the J. C. Bose National Fellowship, grant number SR/S2/JCB-09/2009, and his students whose work is presented in this article. RP thanks CSIR for her fellowship.

REFERENCES

- Bandaru, S., Chakraborty, A., Giri, S., and Chattaraj, P. K. (2012). Toward Analyzing Some Neutral and Cationic Boron-Lithium Clusters (B_xLi_y $x = 2-6$; $y = 1, 2$) as Effective Hydrogen Storage Materials: A Conceptual Density Functional Study. *Int. J. Quantum Chem.* 112, 695–702. doi:10.1002/qua.23055
- Chakraborty, A., Giri, S., and Chattaraj, P. K. (2011). Analyzing the Efficiency of $M N^-(C_2H_4)$ ($M = Sc, Ti, Fe, Ni$; $N = 1, 2$) Complexes as Effective Hydrogen Storage Materials. *Struct. Chem.* 22, 823–837. doi:10.1007/s11224-011-9754-7
- Chattaraj, P. K., and Roy, D. R. (2007). Update 1 of: Electrophilicity index. *Chem. Rev.* 107, PR46–PR74. doi:10.1021/cr078014b
- Chattaraj, P. K., Maiti, B., and Sarkar, U. (2003). Philicity: a Unified Treatment of Chemical Reactivity and Selectivity. *J. Phys. Chem. A* 107, 4973–4975. doi:10.1021/jp034707u
- Chattaraj, P. K., Bandaru, S., and Mondal, S. (2011a). Hydrogen Storage in Clathrate Hydrates. *J. Phys. Chem. A* 115, 187–193. doi:10.1021/jp109515a
- Chattaraj, P. K., Giri, S., and Duley, S. (2011b). Update 2 of: Electrophilicity index. *Chem. Rev.* 111, PR43–PR75. doi:10.1021/cr100149p
- Chen, Z., Wannere, C. S., Corminboeuf, C., Puchta, R., and Schleyer, P. V. R. (2005). Nucleus-independent Chemical Shifts (NICS) as an Aromaticity Criterion. *Chem. Rev.* 105, 3842–3888. doi:10.1021/cr030088+
- Contreras, M., Osorio, E., Ferraro, F., Puga, G., Donald, K. J., Harrison, J. G., et al. (2013). Isomerization Energy Decomposition Analysis for Highly Ionic Systems: Case Study of Starlike $E5Li_7$ +Clusters. *Chem. Eur. J.* 19, 2305–2310. doi:10.1002/chem.201203329
- Dincă, M., Dailly, A., Liu, Y., Brown, C. M., Neumann, D. A., and Long, J. R. (2006). Hydrogen Storage in a Microporous Metal–Organic Framework with Exposed Mn^{2+} Coordination Sites. *J. Am. Chem. Soc.* 128, 16876–16883. doi:10.1021/ja0656853
- Ding, R. G., Lu, G. Q., Yan, Z. F., and Wilson, M. A. (2001). Recent Advances in the Preparation and Utilization of Carbon Nanotubes for Hydrogen Storage. *J. Nanosci. Nanotechnol.* 1, 7–29. doi:10.1166/jnn.2001.012
- Dresselhaus, M. S., Williams, K. A., and Eklund, P. C. (1999). Hydrogen Adsorption in Carbon Materials. *MRS Bull.* 24, 45–50. doi:10.1557/S0883769400053458
- Duley, S., Giri, S., Sathyamurthy, N., Islas, R., Merino, G., and Chattaraj, P. K. (2011). Aromaticity and Hydrogen Storage Capability of Planar and Rings. *Chem. Phys. Lett.* 506, 315–320. doi:10.1016/j.cplett.2011.03.037
- Frisch, M. J., Trucks, G. W., Schlegel, H. B., Scuseria, G. E., Robb, M. A., Cheeseman, J. R., et al. (2003). *Gaussian 03, Revision B. 03*. Pittsburgh, PA: Gaussian, Inc.
- Frisch, M. J., Trucks, G. W., Schlegel, H. B., Scuseria, G. E., Robb, M. A., Cheeseman, J. R., et al. (2009). *Gaussian 09*. Wallingford CT: Gaussian, Inc.
- Froudakis, G. E. (2002). Hydrogen Interaction with Carbon Nanotubes: a Review of *Ab Initio* Studies. *J. Phys. Condens. Matter* 14, R453–R465. doi:10.1088/0953-8984/14/17/201
- Garratt, P. J. (1986). *Aromaticity*. New York: Wiley.
- Giri, S., Roy, D. R., Duley, S., Chakraborty, A., Parthasarathi, R., Elango, M., et al. (2009). Bonding, Aromaticity, and Structure of Trigonal Dianion Metal Clusters. *J. Comput. Chem.* 31, 1815. doi:10.1002/jcc.21452

- Giri, S., Chakraborty, A., and Chattaraj, P. K. (2011a). Potential Use of Some Metal Clusters as Hydrogen Storage Materials-A Conceptual DFT Approach. *J. Mol. Model.* 17, 777–784. doi:10.1007/s00894-010-0761-1
- Giri, S., Chakraborty, A., and Chattaraj, P. K. (2011b). Stability and Aromaticity of $n\text{H}_2@B_{12}N_{12}(n=1-12)$ Clusters. *Nano Rev.* 2, 5767. doi:10.3402/nano.v2i0.5767
- Giri, S., Bandaru, S., Chakraborty, A., and Chattaraj, P. K. (2011c). Role of Aromaticity and Charge of a System in its Hydrogen Trapping Potential and Vice Versa. *Phys. Chem. Chem. Phys.* 13, 20602–20614. doi:10.1039/C1CP21752F
- Hückel, E. (1931a). Quantentheoretische beitra'ge zum benzolproblem I. Die elektronenkonfiguration des benzols und verwandter verbindungen. *Z. Phys. Chem.* 70, 204–286.
- Hückel, E. (1931b). Quantentheoretische beitra'ge zum benzolproblem II. Quantentheorie der induzierten polarita'ten. *Z. Phys. Chem.* 72, 310–337.
- Hückel, E. (1932). Quantentheoretische beitra'gezum problem der aromatischen und ungesa'ttigten Verbindungen. III. *Z. Phys. Chem.* 76, 628–648.
- IEA (2019). Share of World Total Final Consumption by Source. Paris: IEA. Available at: <https://www.iea.org/data-and-statistics/charts/share-of-world-total-final-consumption-by-source-2019> (Accessed September 20, 2021).
- Jana, G., Pal, R., and Chattaraj, P. K. (2018). Hydrogen Storage in Lithium Adsorbed and Polyolithiated (OLi_2) Heteroatom (B, N) Modified (2, 2) γ -graphyne Nanotube and its CO Sensing Potential: A Computational Study. *J. Ind. Chem. Soc.* 95, 1457–1464. Available at: https://www.researchgate.net/profile/Ranita-Pal-2/publication/332497267_Hydrogen_storage_in_lithium_adsorbed_and_polyolithiated_OLi_2_heteroatom_B_N_modified_2_2_graphyne_nanotube_and_its_CO_sensing_potential_A_computational_study/links/60fe9f4a1e95fe241a8bdbde/Hydrogen-storage-in-lithium-adsorbed-and-polyolithiated-OLi-2-heteroatom-B-N-modified-2-2-graphyne-nanotube-and-its-CO-sensing-potential-A-computational-study.pdf.
- Jana, G., Pal, R., Mondal, S., and Chattaraj, P. K. (2020). Do The Ni Binding Modes on $C_{12}N_{12}$ Cluster Influence its H_2 Trapping Capability? *Adv. Mater. Lett.* 11, 20041500. doi:10.5185/amlett.2020.041500
- Kojima, Y., Suzuki, K.-i., Fukumoto, K., Sasaki, M., Yamamoto, T., Kawai, Y., et al. (2002). Hydrogen Generation Using Sodium Borohydride Solution and Metal Catalyst Coated on Metal Oxide. *Int. J. Hydrogen Energ.* 27, 1029–1034. doi:10.1016/S0360-3199(02)00014-9
- Korkin, A. A., Schleyer, P. V. R., and McKee, M. L. (1995). Theoretical Ab Initio Study of Neutral and Charged B_3H_n ($N = 3-9$) Species. Importance of Aromaticity in Determining the Structural Preferences. *Inorg. Chem.* 34, 961–977. doi:10.1021/ic00108a031
- Kubas, G. J. (2001). *Metal Dihydrogen and Bond Complexes-Structure, Theory and Reactivity*. New York: Kluwer Academic/Plenum Publishing.
- Kuznetsov, A. E., and Boldyrev, A. I. (2004). A Single π -bond Captures 2, 3, 4 and 5 Atoms. *Chem. Phys. Lett.* 388, 452–456. doi:10.1016/j.cplett.2004.02.083
- Li, X., Kuznetsov, A. E., Zhang, H.-F., Boldyrev, A. I., and Wang, L.-S. (2001). Observation of All-Metal Aromatic Molecules. *Science* 291, 859–861. doi:10.1126/science.291.5505.859
- Liang, Y., Dai, H.-B., Ma, L.-P., Wang, P., and Cheng, H.-M. (2010). Hydrogen Generation from Sodium Borohydride Solution Using a Ruthenium Supported on Graphite Catalyst. *Int. J. Hydrogen Energ.* 35, 3023–3028. doi:10.1016/j.ijhydene.2009.07.008
- Lochan, R. C., and Head-Gordon, M. (2006). Computational Studies of Molecular Hydrogen Binding Affinities: The Role of Dispersion Forces, Electrostatics, and Orbital Interactions. *Phys. Chem. Chem. Phys.* 8, 1357–1370. doi:10.1039/B515409J
- Minkin, V., Glukhovtsev, M., and Simkin, E. (1994). *Aromaticity and Antiaromaticity. Electronic and Structural Aspects*. New York: Wiley-Interscience.
- Mondal, S., Srinivasu, K., Ghosh, S. K., and Chattaraj, P. K. (2013). Isomers of $C_{12}N_{12}$ as Potential Hydrogen Storage Materials and the Effect of the Electric Field Therein. *RSC Adv.* 3, 6991–7000. doi:10.1039/C3RA00013C
- Pan, S., Giri, S., and Chattaraj, P. K. (2011). A Computational Study on the Hydrogen Adsorption Capacity of Various Lithium-Doped boron Hydrides. *J. Comput. Chem.* 33, 425–434. doi:10.1002/jcc.21985
- Pan, S., Merino, G., and Chattaraj, P. K. (2012). The Hydrogen Trapping Potential of Some Li-Doped star-like Clusters and Super-alkali Systems. *Phys. Chem. Chem. Phys.* 14, 10345–10350. doi:10.1039/C2CP40794A
- Parr, R. G., and Pearson, R. G. (1983). Absolute Hardness: Companion Parameter to Absolute Electronegativity. *J. Am. Chem. Soc.* 105, 7512–7516. doi:10.1021/ja00364a005
- Parr, R. G., and Yang, W. (1984). Density Functional Approach to the Frontier-Electron Theory of Chemical Reactivity. *J. Am. Chem. Soc.* 106, 4049–4050. doi:10.1021/ja00326a036
- Parr, R. G., and Yang, W. (1989). *Density Functional Theory of Atoms and Molecules*. New York: Oxford University Press.
- Parr, R. G., Donnelly, R. A., Levy, M., and Palke, W. E. (1978). Electronegativity: the Density Functional Viewpoint. *J. Chem. Phys.* 68, 3801–3807. doi:10.1063/1.436185
- Parr, R. G., Szentpály, L. V., and Liu, S. (1999). Electrophilicity index. *J. Am. Chem. Soc.* 121, 1922–1924. doi:10.1021/ja983494x
- Pearson, R. G. (1997). *Chemical Hardness*, 10. Weinheim: Wiley VCH. No. 3527606173.
- Peng, Q., Chen, G., Mizuseki, H., and Kawazoe, Y. (2009). Hydrogen Storage Capacity of $C_{60}(\text{OM})_{12}$ ($M=\text{Li}$ and Na) Clusters. *J. Chem. Phys.* 131, 214505. doi:10.1063/1.3268919
- Perez-Peralta, N., Contreras, M., Tiznado, W., Stewart, J., Donald, K. J., and Merino, G. (2011). Stabilizing Carbon-Lithium Stars. *Phys. Chem. Chem. Phys.* 13, 12975–12980. doi:10.1039/C1CP21061K
- Rosi, N. L., Eckert, J., Eddaoudi, M., Vodak, D. T., Kim, J., O'Keeffe, M., et al. (2003). Hydrogen Storage in Microporous Metal-Organic Frameworks. *Science* 300, 1127–1129. doi:10.1126/science.1083440
- Roy, D. R., and Chattaraj, P. K. (2008). Reactivity, Selectivity, and Aromaticity of $\text{Be}_3\text{-2}$ and its Complexes. *J. Phys. Chem. A* 112, 1612–1621. doi:10.1021/jp710820c
- Schleyer, P. V. R., Maerker, C., Dransfeld, A., Jiao, H., and van Eikema Hommes, N. J. R. (1996). Nucleus-independent Chemical Shifts: a Simple and Efficient Aromaticity Probe. *J. Am. Chem. Soc.* 118, 6317–6318. doi:10.1021/ja960582d
- Shevlin, S. A., and Guo, Z. X. (2006). Transition-metal-doping-enhanced Hydrogen Storage in boron Nitride Systems. *Appl. Phys. Lett.* 89, 153104. doi:10.1063/1.2360232
- Srinivasu, K., Chandrakumar, K. R. S., and Ghosh, S. K. (2009). Computational Investigation of Hydrogen Adsorption by Alkali-Metal-Doped Organic Molecules: Role of Aromaticity. *ChemPhysChem* 10, 427–435. doi:10.1002/cphc.200800520
- Srinivasu, K., Ghosh, S. K., Das, R., Giri, S., and Chattaraj, P. K. (2012). Theoretical Investigation of Hydrogen Adsorption in All-Metal Aromatic Clusters. *RSC Adv.* 2, 2914–2922. doi:10.1039/C2RA00643J
- Ströbel, R., Garche, J., Moseley, P. T., Jörissen, L., and Wolf, G. (2006). Hydrogen Storage by Carbon Materials. *J. Power Sourc.* 159, 781–801. doi:10.1016/j.jpowsour.2006.03.047
- Thorn, D. L., and Hoffmann, R. (1979). Delocalization in Metallocycles. *Nouv. J. Chim.* 3, 39–45.
- Tiznado, W., Perez-Peralta, N., Islas, R., Toro-Labbe, A., Ugalde, J. M., and Merino, G. (2009). Designing 3-D Molecular Stars. *J. Am. Chem. Soc.* 131, 9426–9431. doi:10.1021/ja903694d
- U.S. Department of Energy, USCAR (2017). Target Explanation Document: Onboard Hydrogen Storage for Light-Duty Fuel Cell Vehicles. Available: https://www.energy.gov/sites/default/files/2017/05/f34/fcto_targets_onboard_hydrogen_storage_explanation.pdf (Accessed September 20, 2021).
- Wagems, R. W. P., van Lenthe, J. H., de Jongh, P. E., Van Dillen, A. J., and de Jong, K. P. (2005). Hydrogen Storage in Magnesium Clusters: Quantum Chemical Study. *J. Am. Chem. Soc.* 127, 16675–16680. doi:10.1021/ja054569h
- Wang, Q., Sun, Q., Jena, P., and Kawazoe, Y. (2009). Potential of AlN Nanostructures as Hydrogen Storage Materials. *ACS Nano* 3, 621–626. doi:10.1021/nn800815e
- World Nuclear Association Website (2016). Heat Values of Various Fuels. Available at: <https://www.world-nuclear.org/information-library/facts-and-figures/heat-values-of-various-fuels.aspx> (Accessed September 20, 2021).
- Wu, X., Gao, Y., and Zeng, X. C. (2008). Hydrogen Storage in Pillared Li-Dispersed boron Carbide Nanotubes. *J. Phys. Chem. C* 112, 8458–8463. doi:10.1021/jp710022y
- Wu, G., Wang, J., Zhang, X., and Zhu, L. (2009). Hydrogen Storage on Metal-Coated B80 Buckyballs with Density Functional Theory. *J. Phys. Chem. C* 113, 7052–7057. doi:10.1021/jp8113732

- Xu, W., Takahashi, K., Matsuo, Y., Hattori, Y., Kumagai, M., Ishiyama, S., et al. (2007). Investigation of Hydrogen Storage Capacity of Various Carbon Materials. *Int. J. Hydrogen Energ.* 32, 2504–2512. doi:10.1016/j.ijhydene.2006.11.012
- Yildirim, E. K., and Güvenç, Z. B. (2009). A Density Functional Study of Small Li-B and Li-B-H Clusters. *Int. J. Hydrogen Energ.* 34, 4797–4816. doi:10.1016/j.ijhydene.2009.03.051
- Züttel, A., Wenger, P., Rentsch, S., Sudan, P., Mauron, P., and Emmenegger, C. (2003). LiBH₄ a New Hydrogen Storage Material. *J. Power Sourc.* 118, 1–7. doi:10.1016/S0378-7753(03)00054-5

Conflict of Interest: The authors declare that the research was conducted in the absence of any commercial or financial relationships that could be construed as a potential conflict of interest.

Publisher's Note: All claims expressed in this article are solely those of the authors and do not necessarily represent those of their affiliated organizations, or those of the publisher, the editors and the reviewers. Any product that may be evaluated in this article, or claim that may be made by its manufacturer, is not guaranteed or endorsed by the publisher.

Copyright © 2021 Pal and Chattaraj. This is an open-access article distributed under the terms of the Creative Commons Attribution License (CC BY). The use, distribution or reproduction in other forums is permitted, provided the original author(s) and the copyright owner(s) are credited and that the original publication in this journal is cited, in accordance with accepted academic practice. No use, distribution or reproduction is permitted which does not comply with these terms.